

# Plume Separated Region as a Flameholder

James Stark Draper\*

*Aerodyne Research, Inc., Burlington, Mass.*

The luminous flames in the Apollo first stage exhaust flow are considered in terms of the requirements for stabilizing hydrocarbon flames in low pressure, high speed flowfields. Above 12-15 km alt, flame stabilization depends upon a series of recirculation flows about the base of the first stage. Above 30 km alt, the flames are stabilized by the separated body flow (plume separated) region upstream of the expanding exhaust plume flowfield. The hot, fuel rich separated region is bounded by a combustible outer shear layer which contains the luminous flames. As altitude increases, the length  $\ell$  of the nonluminous gap, from the point of separation to the leading edge of the luminous flame-front, increases. At these altitudes heterogeneous heat release processes, involving direct attack on carbon particles by O and O<sub>2</sub>, appear to replace homogeneous two and three-body recombination processes. As a result the chemical relaxation lengths for radical formation and heat release are always smaller than the nonluminous gap length,  $\ell$ . Thus the Apollo body separated region flames are in the same region of "rapid" chemistry as the flame stabilization studies of Zukoski and Marble.<sup>7</sup> After introducing a pressure factor to account for changing heating rates, their "blowoff" criterion is adapted to the variable pressure flame holder in the Apollo flowfield giving:  $p\ell/u \sim 0.5 - 1.5 \times 10^{-4}$  atm-sec, where  $p$  is the separated region pressure, and  $u$  is the exterior stream speed. The flames "blowoff" the Apollo exhaust flow when  $\ell$  attains the length of the plume separated region outer shear layer.

## I. Introduction

IN the high speed flowfields characteristic of rocket flight the luminous flames in the Apollo exhaust must be stabilized by "flameholders." The details of operation of the flameholders are significant for understanding the chemical process occurring throughout the rocket plume flowfield. Typically, most flameholder studies have been carried out at small scales and low flow speeds at atmospheric pressure. Investigation of the Apollo flameholder extends this flame stabilization data base down to pressures of  $2 \times 10^{-3}$  atm, to combustible structures over 100m in length, and to blow-off speeds above  $2 \times 10^3$  m/sec. The Apollo vehicle is particularly suitable for such study, since: 1) it is a very well-documented vehicle, and 2) its first stage fuel is a hydrocarbon for which a most extensive laboratory data base is available on both flame chemistry and flame stabilization.

## II. The Flight Data

Bright orange flames are a well-known feature at the launch of Apollo boosters. These turbulent diffusion flames (based upon atmospheric O<sub>2</sub> diffusing, by turbulent transport, into the fuel rich periphery of the exhaust) are stationary in rocket coordinates. Apparently these same bright orange flames persist to altitudes above 50 km, while undergoing systematic changes in size and location. The sequential development of the flames is shown in Figs. 1 and 2, 6 frames taken from ALOTS Apollo color movie photography. Close examination shows that, for altitudes above 25 km, a cone shaped region upstream of the exit plane is also luminous. The mass of flame is seen to be attached to this cone shaped region through all altitudes. Ultimately, above 50 km, the flames "blow off" this region (as pressure drops and flight speed rises) and the

remainder of the plume altogether. This process is strikingly like "blow-off" of flames from bluff-bodied flameholders of a much smaller size which have been studied in the laboratory.

The Apollo ALOTS films are the principal source of the data studied here. The data extraction and the associated errors require some comment. As supplied by NASA, these films were without time marks or coverage of the moment of launch. A time mark was available in the Apollo S-IC retrorocket firing event which did appear in the films. By use of the Apollo Postflight Trajectory volume<sup>1</sup> and redundant checks on the film framing rate, the Apollo flight speeds and altitudes associated with given frames were determined with an accuracy of better than  $\pm 5\%$ . Flow dimensions were determined to an accuracy of  $\pm 10\%$  using the first stage diameter. Using the projected lengths of the vehicle upper stages, the ALOTS viewing angle  $\phi$  between the vehicle axis and the ALOTS line of sight was determined with an accuracy depending upon the value of  $\phi$ . The data in Figs. 1 and 2 show that at the higher altitude the flame structures are not azimuthally symmetric about the vehicle axis. This azimuthal irregularity leads to a range of "ignition gap" length ( $\ell$ , the distance between the separation point and the flame-front) at one flight condition. It is this range of  $\ell$  that determines the experimental scatter and not the observational errors which are much smaller. This unsymmetric flow is probably due to the base flowfield irregularities resulting from side blowing among the 5 nozzles. The small but finite angles of attack ( $\sim 1^\circ$ )<sup>2</sup> also contribute crossflow effects which disturb the azimuthal regularity of the base flowfield.

Analysis of the plume separated region requires additional information beyond that available in the ALOTS films. This includes plume separated region development, geometrical details, pressures, and temperatures. These have been obtained through use of the calculation procedure of Plotkin.<sup>3</sup> Separated region flow composition has been inferred from optical data taken in the base flow region and calculations of the Apollo first stage LOX/RP-1 F-1 engine exhaust products.<sup>4</sup>

## III. The Flowfield

The separated flows at high altitude are related to the systematic development of the vehicle base region recirculation flows shown in a sketch in Fig. 3 adapted from Wilkinson.<sup>5</sup> This flow region is initially purged with air (Fig. 3a) until the decreasing ambient pressure allows exhaust gases

Presented as Paper 75-243 at the AIAA 13th Aerospace Sciences Meeting, Pasadena, Calif., January 20-22, 1975; submitted January 6, 1975; revision received August 19, 1975. This work was supported by ARPA under ARPA Order 2656, Contract DAAHO1-74-C-0429 monitored by George Drake of AMICOM, Redstone Arsenal, Huntsville, Ala. The author wishes to acknowledge discussions with Dr. Hans Wolfhard of the Institute for Defense Analyses, Dr. Bill Shih of SAI, Inc., Mr. Jim Earle of NASA/MSFC, and Dr. Chuck Kolb of Aerodyne Research, Inc.

Index categories: Reactive Flows; LV/M Aerodynamics; Combustion Stability, Ignition, and Detonation.

\*Member AIAA.

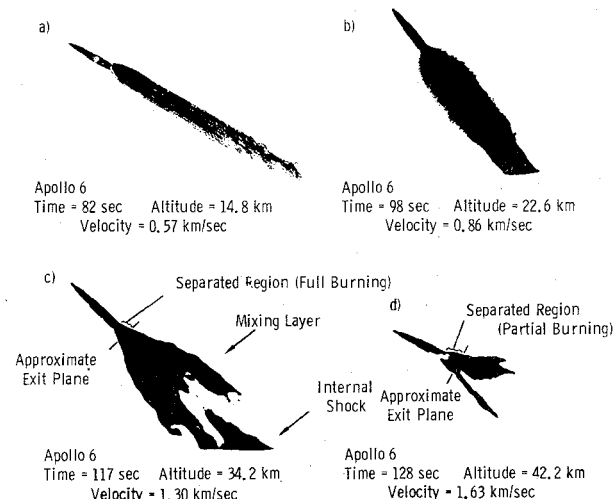


Fig. 1 ALOTS photography of Apollo plumes (courtesy of NASA/MSFC).

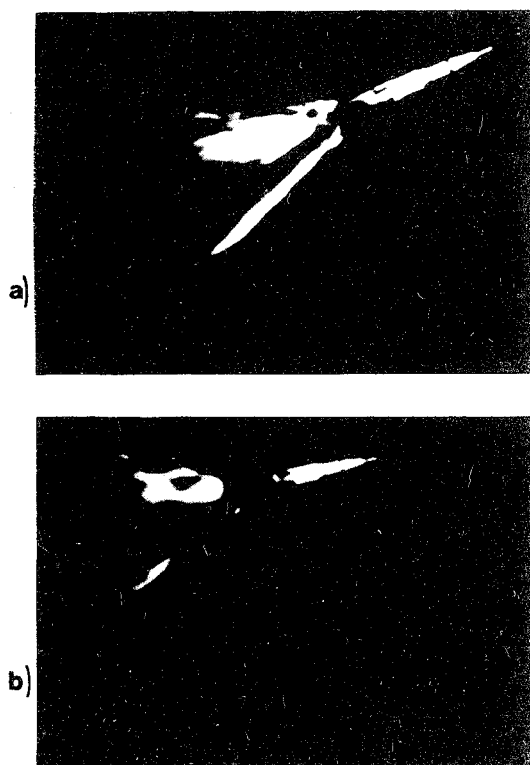


Fig. 2 Luminous flames in the Apollo 6 plume separated region (trajectory data from Ref. 1, and ALOTS data courtesy of NASA/MSFC). a) time=132.5 sec; altitude=45.1 km; and velocity=1.78 km/sec. b) time=140.7 sec; altitude=52.5 km; and velocity=2.09 km/sec.

to turn forward (Fig. 3b). At this point the possibility of combustion in the internozzle region exists since the reentrant gases from the exhaust periphery are fuel rich. This internozzle region combustion will intensify as the plume expands (Fig. 3c) until a separated region forms about the vehicle base ahead of the plume (Fig. 3d). This plume separated region, formed when the vehicle wall boundary-layer momentum is insufficient to overcome the adverse pressure gradient created by the expanding plume, cuts off the atmospheric  $O_2$  mass flow into the internozzle region. As a result, internozzle combustion ceases. Burning can proceed, however, in the combustible outer shear layers of the plume separated region. When the chemical ignition time increases, so as to exceed the available flow residence time (and prevent

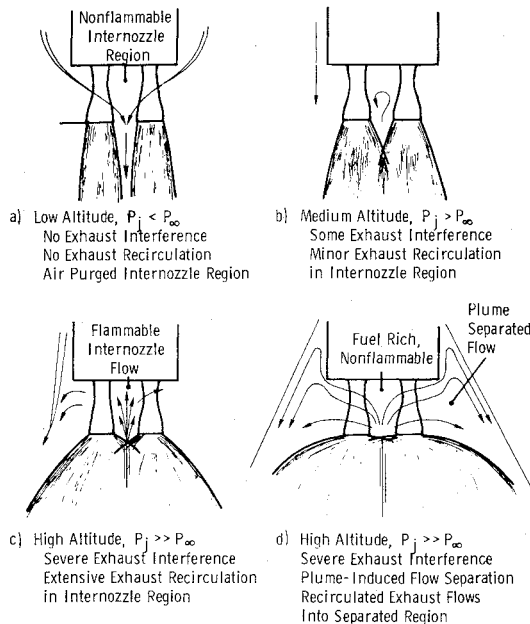


Fig. 3 Exhaust recirculation and plume-induced flow separation.<sup>5</sup>

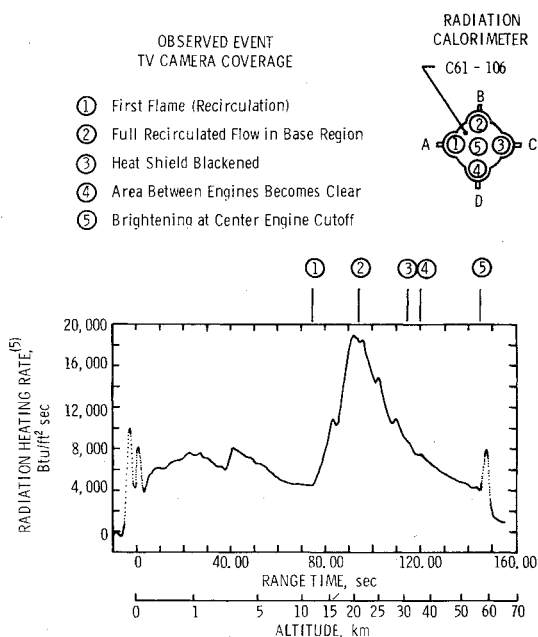


Fig. 4 Comparison of the TV camera coverage and flight data for the Apollo 6 trajectory.<sup>1,6</sup>

ignition), the plume separated region ceases to stabilize the luminous flames. Being the last available flameholder, luminous flames will disappear from the entire plume.

#### Internozzle Flow

At sufficiently high altitudes, the underexpanded nozzle flow expands forward into the 5 engine internozzle volume. Burning with  $O_2$ , entrained from the vehicle boundary-layer flow,<sup>5</sup> commences once the fuel/ $O_2$  mixture ratio rises past the lean flammability limit. When the plume separated region forms, this combustion becomes more fuel rich until it ceases when the mixture ratio exceeds the fuel rich flammability limit. This sequence is shown from heat transfer gauge and TV camera coverage of the Apollo S-IC internozzle volume<sup>6</sup> in Fig. 4. Below 15 km alt, ambient pressure is sufficient to prevent significant exhaust flow into this volume so that heat loads are low and steady while no flames are seen. Simultaneously, of course, extensive burning covers the

plume exterior flow, see Fig. 1a. Abruptly at 12 km alt, the "first flame (recirculation)" (NASA comment<sup>6</sup>) appears coincidentally with a sharp rise in heat loads which peak at 22 km alt. As the plume separated region cuts off  $O_2$ , flow into the internozzle volume combustion becomes fuel rich and eventually ceases. At 30 km alt, the heat shields in the TV camera field of view blacken (with carbon). At 35 km alt, the internozzle region clears of flame and heat loads return to the values seen before internozzle combustion. This potentially combustible, hot exhaust flow is now injected between the nozzles into the plume separated region.

#### Plume Separated Region

The plume separated region and its relation to the Apollo flowfield are shown in Fig. 5. The Apollo vehicle separated region pressures and dimensions have been calculated using the procedure of Plotkin.<sup>3</sup> Over the altitudes of interest (25 to 55 km) the separation angle remains relatively constant between  $11^\circ$  and  $15^\circ$ , while the separated region pressure is a function of freestream Mach number.<sup>3</sup> The flow stagnation temperatures are recovered on the inner edge of the outer shear layer. The composition of the separated zone consists of very hot gases injected from the internozzle volume and entrained from the plume shear layer, and hot combustion products entrained from the outer shear layer. At the lower altitudes the later process helps in maintaining high temperatures (between 1500 K and 2000 K) in the recirculation gases. At the higher altitudes the hot exhaust gases and, to a smaller extent, recovery of freestream conditions in the shear layer will help keep temperatures in this range. So gas temperatures, in excess of hydrocarbon ignition temperatures, are maintained next to the shear layer over the Apollo S-IC flight. That the plume separated region is fuel rich is shown by the blackening (carbon deposition) of the white Apollo vehicle downstream of the separation point in Fig. 2.

#### IV. The Flameholder Model

A series of assumptions are required to clarify the operation of the Apollo plume separated region as a flameholder. This will allow quantitative comparison between the laboratory and field data. Throughout the range of interest the combustion bounding the plume separated region takes place in the well-developed, turbulent outer shear layer. As the separated shear layer originates in a well mixed, small turbulent scale flow it will be assumed that the air and fuel species are well-mixed on the molecular level required for chemical reactions. For example, at the highest altitude where flames are seen (52.5 km), at the separation point the Apollo wall Reynolds number, and boundary layer thickness exceed  $1 \times 10^7$  and 1m, respectively. Burning will be assumed to take place in a thin layer of the turbulent shear layer for which ignition delay is minimal based upon local reactant mixture ratios and temperatures, and for which mixing rates far exceed chemical rates. Moreover, the inner boundary of this shear layer is uniformly hot, with temperatures always in excess of mixture ignition temperatures. This simplified description of the burning flow is similar to descriptions of the premixed, constant pressure flameholder, the operation of which is fairly well understood.

##### The Constant Pressure Flameholder

Hydrocarbon/ $O_2$  flame stabilization has been studied, at 1 atm pressure, in the recirculation zone behind bluff bodies in premixed flows by Zukoski and Marble.<sup>7</sup> They showed that these flows would cease to stabilize flames when the flow approach speed attained its "blow-off" value,  $u_{BO}$ , defined by

$$u_{BO} = L/\tau \quad (1)$$

where  $L$  is the length of the recirculation region downstream of the bluff body, and  $\tau$  is an "ignition time" for a particular

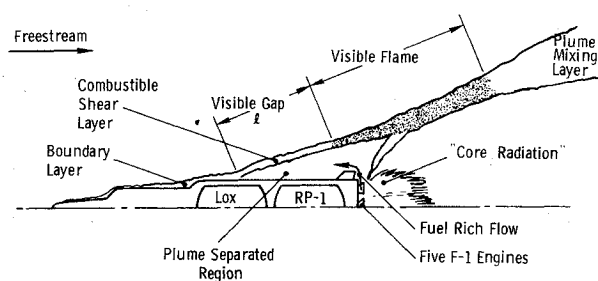


Fig. 5 Plume induced separated flow showing the shear flows and recirculation region at 42 km alt.

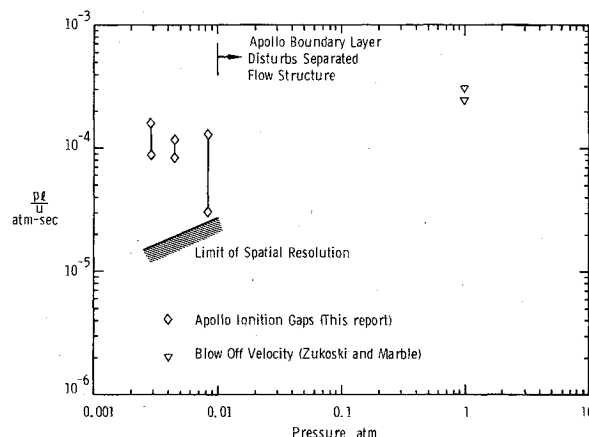


Fig. 6 Comparison of high and low pressure flame stabilization in hydrocarbon systems.

chemistry and fuel-air equivalence ratio. All recirculation region combustion is restricted to the outer shear layer. For ignition, and a stable flame, the shear layer residence time (not the recirculation flow residence time) must exceed the chemical ignition time. In the bluff body flameholders, high recirculation region temperatures are maintained entirely by entrainment of hot combustion products up to flame blow-off.

There is a close correspondence (in chemistry, flow geometry, and temperature) between the 1 atm bluff body flows of Zukoski and Marble and the Apollo vehicle separated flows. There is also a very important difference: the pressure in the Apollo separated region drops to  $\sim 2 \times 10^{-3}$  atm. It is necessary to reconsider: 1) whether the combustion chemistry rates at low pressure are still faster than the observed ignition times, and 2) the effect of pressure on the flame stabilization criterion in Eq. (1).

##### Chemistry: Homogeneous and Heterogeneous

The observed flames involve combustion of  $H_2$  and CO in an oxygen and carbon particle environment. There are 2-body radical ( $H$ ,  $OH$ ,  $O$ ) formation and 3-body heat release processes. First consider a radical formation process. From Jensen and Wilson<sup>8</sup> the attack on  $O_2$  by  $H$  is



where the rate is

$$k_1 = 3.7 \times 10^{-10} \exp(-8400/T) \text{ cm}^3 \text{ sec}^{-1} \quad (3)$$

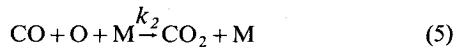
The chemical rate for  $OH$  formation is

$$\frac{1}{\tau_{OH}} \equiv k_1 [O_2] \text{ sec}^{-1} \quad (4)$$

Consider the extreme altitude at which flames are seen, about 52.5 km. At a point in the shear layer where its temperature is about 1550 K, its mean speed is about 500 m/sec. The mole

fraction of  $O_2$  diffusing into this region is about  $10^{-2}$ . The light radicals diffuse sufficiently rapidly toward the origin of the shear layer to maintain the flame. The chemical time is  $\tau_{OH} \sim 12$  msec and length is  $u \tau_{OH} \sim 6$  m. This is small compared to the 60-100 m ignition gap seen at this altitude. Two body rates in the gas phase do not determine the ignition delay in either the Zukoski and Marble or the Apollo vehicle flows.

At high pressures, heat release is by gas phase recombination processes such as<sup>8</sup>



for which the rate is

$$k_2 = 1 \times 10^{-29} \exp(-1250/T) / T \text{ cm}^6 \text{ sec}^{-1} \quad (6)$$

$$\frac{I}{\tau_{CO_2}} \equiv k_2 [CO] [M] \text{ sec}^{-1} \quad (7)$$

Using the same combustion zone species mole fractions as for  $\tau_{OH}$  and as in Pergament and Calcote,<sup>9</sup> the characteristic time for 3-body recombination at 42.2 km is  $\tau_{CO_2} \sim 5$  sec. This time far exceeds the flow times available ( $u \tau_{CO_2} \sim 2.5$  km). The luminous flames in Fig. 2 (and even Fig. 1) cannot depend, for heat release, upon gas phase, homogeneous 3-body recombination.

For the studies of Zukoski and Marble, the characteristic chemical lengths for gas phase 3-body recombination are always much smaller than the recirculation flow lengths. Flame stabilization was not determined by chemical rates. To continue the comparison in this paper between their results and the Apollo flame stabilization, it is first necessary to demonstrate that recombination processes are sufficiently fast in the Apollo case. Fuel rich LOX/RP-1 rocket exhausts are known to contain appreciable carbon particle mass fractions.<sup>†</sup> As an alternative to gas phase recombination, heterogeneous gas-surface reactions by these particles requires evaluation.

For the conditions of the F-1 peripheral exhaust flow it is estimated that carbon particle mass fractions exceed 5% by weight and that the mean particle diameter is  $\sim 0.03 \mu\text{m}$ . The rates for molecular and atomic oxygen recombination on these particles will be considered for the Apollo vehicle at 52.5 km altitude. Here the interparticle separation and mean free paths are both comparable to  $10^{-2}$  cm so that molecular transport to the particle surface can be estimated from kinetic flux

$$\Gamma_i = [i] \bar{c}_i / 4 \quad (8)$$

where  $[i]$  is the concentration of species  $i$ , and  $\bar{c}_i$  is the mean thermal speed of species  $i$ .

The total flux of species  $i$  to the total particle surface area per unit volume is  $\Gamma_i 4\pi r^2 N_p$ , where  $r$  is particle radius, and  $N_p$  is number of particles per unit volume. The total number of reactions of gas phase species  $i$  with solid phase species  $j$  resulting in bound species  $ij$  per unit time per unit volume is

$$\frac{d[ij]}{dt} = \sum_i F_i \Gamma_i 4\pi r^2 N_p \quad (9)$$

where  $F_i$  is the probability of the reaction resulting in new species  $ij$ . The characteristic reaction time is

$$\frac{I}{\tau_{CO}} \equiv \frac{d\dot{m}[CO]}{dt} = \left[ F_O \frac{[O]}{[CO]} \frac{\bar{c}_O}{4} + 2F_{O_2} \frac{[O_2]}{[CO]} \frac{\bar{c}_{O_2}}{4} \right] 4\pi r^2 N_p \quad (10)$$

<sup>†</sup> Estimates place the Apollo first stage gas generator flows at 40% by weight of particles. This total flow rate, of 850 lb/sec, is injected into the nozzle skirts and therefore directly into the recirculation regions discussed here.

For  $O + C(s) \rightarrow CO$  it has been shown that  $F_O \sim 0.3$  for particle temperatures of 1000 K to 1500 K. The CO very rapidly desorbs from the carbon. For  $O_2 + C(s) \rightarrow 2 CO$  the corresponding  $F_{O_2}$  is  $1.6 \times 10^{-2}$ . These results are from the molecular beam studies of Shih<sup>10</sup> and Liu.<sup>11</sup> As a result  $\tau_{CO} \sim 10$  msec. The characteristic chemical length for this reaction process is  $\sim 5$  m, much shorter than the ignition gaps  $\ell$  seen in the Apollo shear layer. The important chemical characteristic lengths  $u_\infty \tau_i$  are much smaller than the ignition gaps, and the Apollo flameholder is in the same "fast" chemical regime as those studied by Zukoski and Marble. Inclusion of the  $CO + OH \rightarrow CO_2 + H$  reaction will only speed up the heat release process somewhat.

### The Variable Pressure Flameholder

As pressure decreases, the operation of the flameholder, even in the fast chemical regime, may change substantially. Khitrin<sup>12</sup> has theoretically considered ignition in a fast, combustible, turbulent boundary layer moving over a hot body. This describes the Apollo flameholder. Khitrin obtains the scaling for the distance  $\ell$  from the origin of the boundary layer to the ignition point (first appearance of flame) as a function of freestream speed  $u$ , gas transport properties, and flame speed  $S$ , as

$$\ell = (k / \pi C_p \rho) / (u / S^2) \quad (11)$$

where  $k$  is thermal conductivity,  $\rho$  is density, and  $C_p$  is the specific heat of the combustion products at constant pressure. If all dependencies upon temperature are grouped into a modified flame speed, then

$$\ell / u \propto 1 / p \quad (12)$$

The similarity of the reacting layer temperatures (i.e., in the Zukoski and Marble and the Apollo vehicle systems) has allowed substitution of  $p$  for  $\rho$ , and the chemical similarities have allowed the modified flame speeds in each system to be assumed to be approximately identical. At the blow-off speed  $L/u$  is the ignition delay of Zukoski and Marble. The variable pressure flameholder operation can be written as

$$p\ell / u \sim 2.4 - 3.1 \times 10^{-4} \text{ atm} - \text{sec} \quad (13)$$

based upon their results in the  $O_2$ /hydrocarbon system at 1 atm. When the ignition gas  $\ell$  attains the recirculation region length  $L$  the flame will "blow-off."

The group  $p\ell/u$ , from the Zukoski and Marble data at 1 atm, and from the lower pressure Apollo vehicle data, is shown in Fig. 6 vs flameholder pressure. The uncertainty errors in the  $\ell$  measurement (smallest resolved distance) are converted to a  $p\ell/u$  values and plotted in Fig. 6 to show that observational errors do not determine the scatter in  $p\ell/u$ . The scatter in the Apollo data originates in the irregular ignition gaps which themselves are due to its azimuthally unsymmetric base flowfield and cross-flow effects. The Apollo data from altitudes below 35 km are not included as the vehicle boundary-layer thickness is comparable to the plume separated region thickness. The correspondence of the values of  $p\ell/u$  from the Apollo data to the Zukoski and Marble results at  $2.4 - 3.1 \times 10^{-4}$  atm-sec at much higher pressures is satisfactory. The differences observed between these measurements are most probably due to: 1) differences in final flame temperatures ( $S \propto \exp(-E/2RT_f)$ ) due to detailed variations in chemistry, and 2) approximations made in the derivation of Khitrin and application of these results to the Apollo outer shear layer ignition.

### V. Conclusions

The luminous flames seen in the Apollo flowfield at high altitudes are stabilized by the combustible outer shear layers bounding the plume separated region. Heterogeneous gas sur-

face processes, catalyzed by carbon particles, maintain sufficiently fast combustion reaction rates. As a result combustion reactions are sufficiently fast for flames to appear throughout the shear layer, even to 52.5 km alt, where they "blow off" the Apollo plume. Both the Apollo and 1 atm pressure, bluff body flameholder conditions are in the regime of "fast" chemistry in which chemical relaxation lengths are much smaller than the observed ignition gaps. Application of the high pressure, bluff body blow-off speed criterion (once similarity in chemical and flowfield conditions has been established) does not predict the correct blow-off speed for the Apollo. For example, at 52.5 km the shear layer is about 100m in length, requiring a blow-off speed of  $3 \times 10^5$  m/sec, based upon the Zukoski and Marble criterion. The observed blow-off speed is closer to  $2 \times 10^3$  m/sec. The reduced blow-off speed is due to the reduced shear layer heating rates at reduced pressure as has been shown using the treatment of Khitrin. There results a scaling law for the variable pressure flameholder which works well over a wide range of flow conditions, including speeds from 10 to 2000 m/sec, pressures from  $2 \times 10^{-3}$  to 1 atm, and sizes from several cm to 100m.

### References

- <sup>1</sup>"Apollo/Saturn V Postflight Trajectory AS-502," Rept. D5-15773, July 31, 1968, George C. Marshall Space Flight Center, Huntsville, Ala.
- <sup>2</sup>"Saturn V/Flight Manual AS-506," Rept. MSFC-MAN-506, Feb. 25, 1969, George C. Marshall Space Flight Center, Huntsville, Ala.

<sup>3</sup>Plotkin, K. J., "Prediction of Fluctuating Pressure Environments Associated with Plume Induced Flowfields," Prog. No. 73/003P-1, May 1973, WR 73-3 Wyle Labs., El Segundo, Calif.

<sup>4</sup>Larson, V. R., F-1 Rocket Engine Exhaust Species Calculations, Rocketdyne/North American Rockwell, March 15, 1972, private communication.

<sup>5</sup>Wilkinson, C. L., "Heat Transfer Within Plume-Induced Flow Separation Region on Saturn V," ASME Paper 69-WA/HT-18, Nov. 1969.

<sup>6</sup>Mullen, C. R., Bender, R. L., Berrill, R. L., Reardon, J., and Hartley, L., "Saturn Base Heating Handbook," NASA CR-61390, May 1, 1972.

<sup>7</sup>Zukoski, E. E. and Marble, F. E., "Proceedings of the Gas Dynamics Symposium on Aerothermochemistry," Northwestern University Press, pp. 205-210.

<sup>8</sup>Jensen, D. E. and Wilson, A. S., *Combustion and Flame*, Vol. 25, Aug. 1975, pp. 43-55.

<sup>9</sup>Pergament, H. S. and Calcote, H. F., "Thermal and Chemionization Processes in Afterburning Rocket Exhausts," 11th Symposium (International) on Combustion (1967), pp. 597-611.

<sup>10</sup>Shih, W. C. C., "Molecular Beam Studies of Graphite Oxidation," Ph.D. thesis, 1973, Massachusetts Institute of Technology, Cambridge, Mass.

<sup>11</sup>Liu, G. N-K., "High Temperature Oxidation of Graphite by a Dissociated Oxygen Beam," Ph.D. thesis, Massachusetts Institute of Technology, Aeronautics and Astronautics Dept., Aug. 1973, Cambridge, Mass.

<sup>12</sup>Khitrin, L. N., "On Some Consequences of the Thermal Theory of Ignition in a Fast Flow," 7th Symposium (International) on Combustion (1958), pp. 470-474.

## *From the AIAA Progress in Astronautics and Aeronautics Series . . .*

### **SPACE POWER SYSTEMS ENGINEERING—v. 16**

*Edited by George C. Szego, Institute for Defense Analyses, and J. Edward Taylor, TRW Inc.*

The sixty-two papers in this volume concern electric power systems for space vehicles, covering requirements and applications, nuclear system development, chemical system development, and MHD power systems.

Papers treat radioisotope power systems, the SNAP series of reactors, nuclear propulsion systems, electric propulsion systems, a comparison and combination of both for space missions, and an optimized nuclear-electric system.

Solar cell power systems are optimized and compared with solar-thermionic systems and Brayton-cycle solar dynamic systems, all of which are posited for specific space missions. Fuel cells systems are analyzed and compared. Rankine cycle generators are proposed for specific applications.

Solar concentrators for power generation are proposed and evaluated, with applications to both Rankine and Brayton cycle conversion systems. Thermionic converters are examined and modeled.

Other papers examine fuel cell chemistry and engineering. Various cells, using various power sources, are considered. Batteries of various types are considered for use with fuel cell systems, and various control systems are proposed.

*1302 pp., 6 x 9, illus., \$29.50 Mem. & List*

TO ORDER WRITE: Publications Dept., AIAA, 1290 Avenue of the Americas, New York, N. Y. 10019